



Reliability Analysis of a Home-scale Microgrid Based on a Threshold System

Taufal Hidayat¹ and Ali Muhammad Rushdi^{2*}

¹*Department of Electrical and Computer Engineering, Faculty of Engineering, King Abdulaziz University, Jeddah, 21589, Saudi Arabia.*

²*Electrical and Computer Engineering, King Abdulaziz University, P.O.Box 80204 Jeddah 21589, Saudi Arabia.*

Authors' contributions

This work was carried out in collaboration between the two authors. Author TH performed the initial analysis, solved the example, wrote the first draft of the manuscript and initiated the literature search. Author AMR envisioned and designed the study, corrected the example solution, added the reliability computations and illustrations, managed the literature search, wrote many parts of, and substantially edited and improved the entire manuscript. Both authors read and approved the final manuscript.

Article Information

DOI: 10.9734/JENRR/2021/v7i330192

Editor(s):

(1) Dr. Inayatullah Jan, the University of Agriculture Peshawar, Pakistan.

Reviewers:

(1) Stephen Ndubuisi Nnamchi, Kampala International University, Uganda.

(2) M Karthigai Pandian, Sri Krishna College of Technology, India.

Complete Peer review History: <http://www.sdiarticle4.com/review-history/67300>

Original Research Article

Received 27 January 2021

Accepted 03 April 2021

Published 12 April 2021

ABSTRACT

The reliability of a microgrid power system is an important aspect to analyze so as to ascertain that the system can provide electricity reliably over a specified period of time. This paper analyzes a home-scale model of a microgrid system by using the threshold system model (inadvertently labeled as the weighted k-out-of-n:G system model), which is a system whose success is treated as a threshold switching function. To analyze the reliability of the system, we first proved that its success is a coherent threshold function, and then identified possible (non-unique) values for its weights and threshold. Two methods are employed for this. The first method is called the unity-gap method and the second is called the fair-power method. In the unity-gap method, we utilize certain dominations and symmetries to reduce the number of pertinent inequalities (turned into equations) to be solved. In the fair-power method, the Banzhaf index is calculated to express the weight of each component as its relative power or importance. Finally, a recursive algorithm for computing system reliability is

*Corresponding author: E-mail: arushdi@kau.edu.sa, arushdi@ieee.org, alirushdi@gmail.com;

presented. The threshold success function is verified to be shellable, and the non-uniqueness of the set of weights and thresholds is demonstrated to be of no detrimental consequence, as different correct sets of weights and threshold produce equivalent expressions of system reliability.

Keywords: Micro grid; k-out-of-n G system; threshold system; Banzhaf index; unity-gap; fair-power; shell ability; probability map.

1. INTRODUCTION

The renewable energy paradigm gained an increasing interest all over the world in the past few years due to the economic, depletion and environmental concerns about fossil fuels. Many renewable forms of energy such as energies produced by wind turbines, airborne wind-energy systems and photovoltaic cells can be considered collectively a viable option for future electricity generation that reduces the impact of the environmental problem of global warming and also mitigates the inevitably forthcoming depletion of the resources of conventional fossil fuels. Moreover, the afore-mentioned types of renewable energy allow the installation of small-capacity generating stations near geographically-sparse consumers, a fact that results in the introduction of the concept of a microgrid [1,2].

The International Electro-technical Commission defines a microgrid in an electric power system as a group of interconnected loads and distributed energy resources with defined electrical boundaries forming a local electric power system at distribution voltage levels, that acts as a single controllable entity and is able to operate in either grid-connected or island mode [3,4]. This definition covers both (utility) distribution microgrids and (customer owned) facility microgrids. It stresses that a microgrid is a decentralized group of electricity sources and loads, in contrast to a macrogrid (a traditional wide area synchronous grid). The definition also indicates that a microgrid normally operates connected to and synchronous with a macrogrid, but it can also be disconnected from the macrogrid to function as an autonomous, stand-alone, off-grid, or isolated microgrid, i.e., in a mode of operation usually referred to as 'island mode.'

The main challenges for the supply of renewable energy through the sources of a microgrid are blackouts and power quality problems. A microgrid based on renewable energy sources, such as wind and solar power, is not stable due to the intermittent generation of power by such sources, due to their critical dependence on the weather conditions, which are typically subject to dramatic variations. This means that these

sources are not reliable as continuous or baseline power supply systems. Therefore, there is a need to assess the reliability of configurations of sources in a microgrid as a means to produce a reliable electric power supply.

There are many methods to analyze the reliability of a microgrid [5–11]. Some authors use fault-tree analysis, Monte Carlo simulation, and Bayesian simulation to evaluate the various types of configurations of a microgrid system. A few methods for system reliability calculation use deterministic rather than probabilistic techniques, thereby suffering from grave lack of accuracy that is due to the inherent stochastic nature of many system components [12].

This paper focuses on the analysis of the reliability of a home-scale (also known as residential-scale, small-scale, or household-scale) microgrid system that is fed by a photovoltaic panel with a diesel generator and a battery as redundant sources. A threshold system (also known as a weighted k-out-of-n:G system) is used as a model to analyze the effect of the given redundancy on the total reliability performance. The rest of the paper has the following organization. Section 2 is a brief introduction to the threshold (weighted k-out-of-n:G) system. Section 3 presents the system modeling of a home-scale microgrid. Section 4 presents the reliability analysis based on the threshold system model. The analysis uses two methods to obtain the (non-unique) threshold and weights of the system success and to find the Banzhaf indexes that fairly represent the importance of each component, Section 5 describes a recursive algorithm for computing system reliability, and verifies that a threshold function is shellable. Though the weights and threshold for the threshold system are not unique, they are found to yield the same expression for system reliability. Section 6 concludes the paper.

2. THRESHOLD (WEIGHTED k-out-of-n:G) SYSTEM

The k-out-of-n:G system is a coherent symmetric reliability system, which works properly if at least

k out of its n components function properly. We note that the probability of exactly k successes out of n is given by [12–15]

$$E(k, n, p) = \binom{n}{k} p^k (1 - p)^{n-k} \quad (1a)$$

where p is the probability of success of a single component. Hence, the reliability of a k-out-of-n:G system with independent identically-distributed components is [14]

$$R(k, n, p) = \sum_{m=k}^n E(m, n, p) \quad (1b)$$

The k-out-of-n G system is the special coherent symmetric case of a threshold system which is a system that is composed of n statistically independent 2-state components whose success is a threshold switching function [16-21]. A switching function is a threshold function (denoted by $H(n; X; W; T)$) if there exists a set of real numbers W_1, W_2, \dots, W_n , called weights and T called a threshold. such that

$$S(X) = 1 \text{ iff } \sum_{i=1}^n W_i X_i \geq T \quad (2)$$

If all the weights are positive and equal, the system is called a k-out-of-n: G system. Otherwise, if the weights are different, it is (sometimes) called a weighted k-out-of-n: G system. A normalization (unity-gap) criterion is usually employed in the selection of the weights of a coherent threshold function. This condition involves the weight input summation [16]

$$F(X) = \sum_{i=1}^n W_i X_i \quad (3)$$

This criterion necessitates that $F(X)$ has its minimum value for true vectors of the function (X such that $S(X) = 1$) exactly equal to one plus its maximum value for false vectors of the function (X such that $S(X) = 0$). This criterion serves as a basis of the unit-gap method in Section 4.

The threshold (weighted k-out-of-n: G system)

has been successfully applied as a system model in many situations. Lu and Liu [15] used the 8-out-of-10: G system to analyze STATCOM devices in electric power systems. Erylmaz [22] used a weighted k-out-of-n: F system to analyze the processing and controlling of a modern engineering system that consists of independent and non-identical components. Zhuang et al. [23] used a weighted k-out-of-n: G system to analyze a combined heat and power system. The system consists of four combined heat and power units where each unit can produce both electrical power and thermal power to the consumer. Song et al. [24] applied the weighted k-out-of-n: G system into transmission line analysis. In their paper, a stochastic multiple-valued (SMV) approach is proposed to predict the reliability of two models of the system with non-repairable components and dynamically repairable components. The threshold-system model seems to be a very convenient model for exploring the reliability of renewable energy sources employing air-borne wind-energy vehicles [25-28].

2.1 System Modeling

The microgrid system is designed to supply a home-scaled load. The system consists of solar energy sources as the main power sources. A battery is used as an alternative power supply and a diesel generator is utilized as a backup power supply. The load is primarily supplied by the photovoltaic source at and around noon time through an inverter to convert dc power, which is produced by the solar power, to ac power that supplies the load. Whenever solar power is too weak (e.g., immediately after sunrise or few hours before sunset, as well as during a cloudy day), or totally missing (e.g., at night), the battery is expected to take over. The secondary energy source (the diesel generator) is used as a back up to supply the load and also charge the battery through a rectifier. The schematic of the system is shown in Fig. 1.

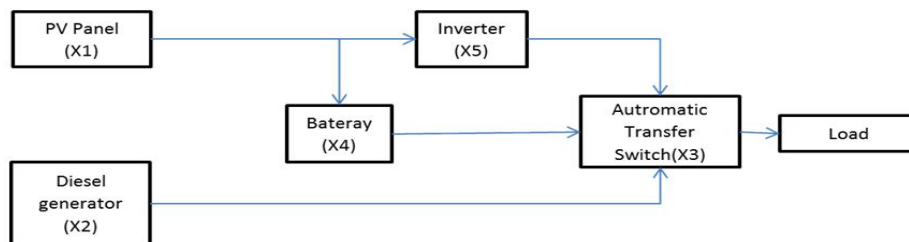


Fig. 1. Block diagram of a Home-scale microgrid system

2.2 Reliability Analysis

In this section, the analysis will proceed by using two methods, borrowed from Rushdi and Alturki [17] to derive the weights and threshold of the microgrid system (assuming they exist). The first method is called the unit-gap method and the second method is called the fair-power method. The unit gap method will be used to find the pseudo-Boolean function of the microgrid system, while the fair power method is used to find the relative importance of each unit of the systems.

a) The Unit-gap Method

The Boolean function of success for the system depicted by the block diagram of Fig. 1 is given by

$$f(X_1, X_2, X_3, X_4, X_5) = X_2 X_3 \vee X_1 X_3 X_5 \vee X_1 X_3 X_4 = X_3 (X_2 \vee X_1 (X_5 \vee X_4)) \quad (4)$$

Correspondingly, its complement, the Boolean function of failure is given by [12, 29-32]

$$\bar{f}(X_1, X_2, X_3, X_4, X_5) = \bar{X}_3 \vee \bar{X}_1 \bar{X}_2 \vee \bar{X}_2 \bar{X}_4 \bar{X}_5 \quad (4a)$$

Note that each of the success and failure functions is partially symmetric in X_4 and X_5 , and hence we set $W_4 = W_5$. The Karnaugh maps of $f(X_1, X_2, X_3, X_4, X_5)$ in Fig. 2 display the true and false cells (vectors) of this function. This figure also highlights in yellow the all-1 cell ($X_1 X_2 X_3 X_4 X_5$) and the all-0 cell ($\bar{X}_1 \bar{X}_2 \bar{X}_3 \bar{X}_4 \bar{X}_5$). Thanks to coherency, these two cells are a true cell and a false cell, respectively. The figure also locates the cells $\{\bar{X}_1 X_2 X_3 \bar{X}_4 \bar{X}_5, X_1 \bar{X}_2 X_3 \bar{X}_4 X_5, X_1 \bar{X}_2 X_3 X_4 \bar{X}_5\}$ that are farthest from the all-1 cell within the prime implicants of system success $\{X_2 X_3, X_1 X_3 X_5, X_1 X_3 X_4\}$, and the cells $\{X_1 X_2 \bar{X}_3 X_4 X_5, \bar{X}_1 \bar{X}_2 X_3 X_4 X_5, X_1 \bar{X}_2 X_3 \bar{X}_4 \bar{X}_5\}$ that are farthest from the all-0 cell within the prime implicants of system failure $\{\bar{X}_3, \bar{X}_1 \bar{X}_2, \bar{X}_2 \bar{X}_4 \bar{X}_5\}$. Rushdi and Alturki [17] have shown that the inequality associated with each of these cells dominates the inequalities within the encompassing prime implicant. Therefore, it suffices to retain only the six dominating inequalities (See Fig. 3 and Table 1). Due to the equality ($W_4 = W_5$), we are left with 5 unknowns to determine.

The calculation process for the five unknowns W_1, W_2, W_3, W_4 and T goes as follows. First, we note that the inequality $W_1 + W_3 + W_4 \geq T$

appears twice, which means that we have five inequalities only. These five inequalities are turned into five independent equations in the remaining five unknowns as follows. The remaining non-strict inequalities (\geq) are satisfied as equations.

$$W_2 + W_3 = W_1 + W_3 + W_4 = T$$

while each of the strict inequalities ($<$) is satisfied as an equation by subtracting a unity gap from the right-hand side

$$W_3 + 2W_4 = W_1 + W_2 + 2W_4 = W_1 + W_3 = T - 1$$

To solve the resulting system of equations, we might use any method for solving a matrix equation. Here, we employ a detailed elimination process. First we note that

$$T = W_1 + W_3 + W_4 = W_1 + W_3 + 1, \text{ so } W_4 = 1$$

The five equations reduce to

$$\begin{aligned} W_2 + W_3 &= W_1 + W_3 + 1 = T \\ W_3 + 2 &= W_1 + W_2 + 2 = W_1 + W_3 = T - 1 \end{aligned}$$

and hence

$$T = W_2 + W_3 = W_3 + 3, \text{ so } W_2 = 3$$

Now, the equations reduce to

$$\begin{aligned} 3 + W_3 &= W_1 + W_3 + 1 = T \\ W_3 + 2 &= W_1 + 5 = W_1 + W_3 = T - 1 \end{aligned}$$

and hence

$$T = W_1 + W_3 + 1 = W_3 + 3, \text{ so } W_1 = 2$$

Finally, the equations reduce to a consistent system of 5 equations in the remaining 2 unknowns

$$3 + W_3 = 2 + W_3 + 1 = T$$

$$W_3 + 2 = 7 = 2 + W_3 = T - 1$$

$$\text{So, } W_3 = 5, T = 8$$

Finally, the threshold $T = 8$ and a possible set of weights is $\{2, 3, 5, 1, 1\}$. An offshoot of this calculation is the proof that our system is threshold, indeed.

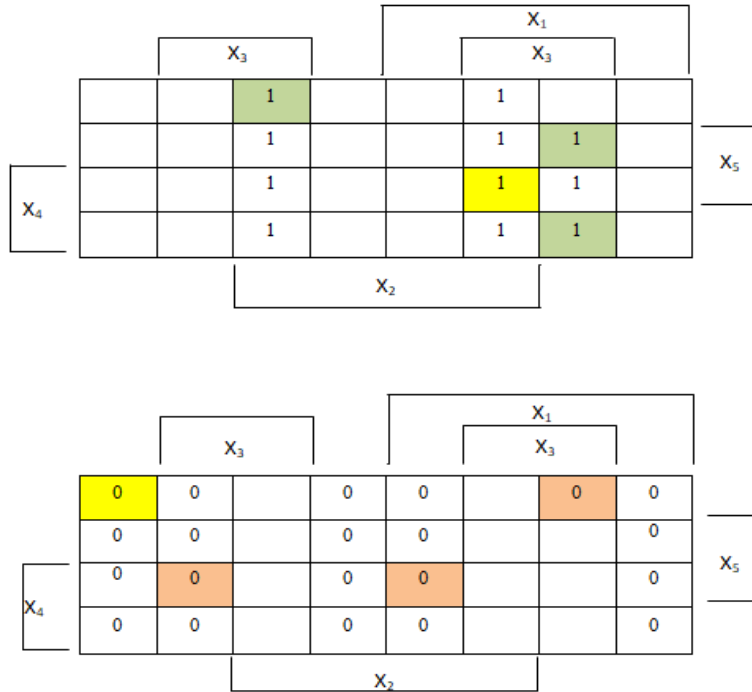


Fig. 2. True and false cells of the success function of the system represented by the block diagram of Fig. 1. The figure identifies the all-1 cell and all true cells farthest from it (to be called critical true cells), and the all-0 cell and all false cells farthest from it (to be called critical false cells)

	X_3		X_1				
			X_3				
		1		1	1		
		1		1	1	1	
X_4		1		1	1	1	
		1		1	1	1	
	X_2						

	X_3		X_1				
			X_3				
	0	0	0	0	0	0	0
	0	0	0	0	0	0	0
X_4	0	0	0	0	0	0	0
	0	0	0	0	0	0	0
	X_2						

	X_3		X_1					
	$0 < T$	$W_3 < T$	$W_2 + W_3 \geq T$	$W_2 < T$	$W_1 + W_2 < T$	$W_1 + W_2 + W_3 \geq T$	$W_1 + W_3 < T$	$W_1 < T$
	$W_5 < T$	$W_3 + W_5 < T$	$W_2 + W_3 + W_5 \geq T$	$W_2 + W_5 < T$	$W_1 + W_2 + W_5 < T$	$W_1 + W_2 + W_3 + W_5 \geq T$	$W_1 + W_3 + W_5 \geq T$	$W_1 + W_5 < T$
X_4	$W_4 + W_5 < T$	$W_3 + W_4 + W_5 < T$	$W_2 + W_3 + W_4 + W_5 \geq T$	$W_2 + W_4 + W_5 < T$	$W_1 + W_2 + W_4 + W_5 < T$	$W_1 + W_2 + W_3 + W_4 + W_5 \geq T$	$W_1 + W_3 + W_4 + W_5 \geq T$	$W_1 + W_4 + W_5 < T$
	$W_4 < T$	$W_3 + W_4 < T$	$W_2 + W_3 + W_4 \geq T$	$W_4 + W_2 < T$	$W_1 + W_2 + W_4 < T$	$W_1 + W_2 + W_3 + W_4 \geq T$	$W_1 + W_3 + W_4 \geq T$	$W_1 + W_3 + W_4 < T$
	X_2							

Fig. 3. The 32 inequalities for the weights and threshold for the running example. These inequalities are written with the (\geq) operator for true vectors and with the ($<$) operator for false vectors. We retain only the 6 highlighted inequalities since they dominate the rest

Table 1. The six dominating inequalities for the running example

Dominating inequality	Exhausts	Symmetry of X_4 and X_5
True (on) Cells		
$W_2 + W_3 \geq T$	Success Prime Implicant X_2X_3	$W_2 + W_3 \geq T$
$W_1 + W_3 + W_4 \geq T$	Success Prime Implicant $X_1X_3X_5$	$W_1 + W_3 + W_4 \geq T$
$W_1 + W_3 + W_5 \geq T$	Success Prime Implicant $X_1X_3X_4$	$W_1 + W_3 + W_4 \geq T$
False (Off) Cells		
$W_3 + W_4 + W_5 < T$	Failure Prime Implicant $\overline{X_1} \overline{X_2}$	$W_3 + 2W_4 < T$
$W_1 + W_2 + W_4 + W_5 < T$	Failure Prime Implicant $\overline{X_3}$	$W_1 + W_2 + 2W_4 < T$
$W_1 + W_3 < T$	Failure Prime Implicant $\overline{X_2} \overline{X_4} \overline{X_5}$	$W_1 + W_3 < T$

b) The Fair Power Method

This sub-section calculates the Banzhaf index for each of the components, which is a measure of the relative importance of the component. The calculation follows the map method shown in Fig. 4 [33-35]. This method uses map folding to ‘differentiate’ the switching function of success [30] and then calculates the weight (the number of true vectors) of the obtained ‘derivative’ [31]. This method discovers the symmetry in X_4 and X_5 , instead of pre-supposing it. It assigns the Banzhaf indexes as weights to the components whether the system is threshold or not. Then it checks if the system is ‘linearly separable’ or not by computing the following pseudo-Boolean function, which employs the weights deduced in Fig. 4.

$$F(X) = 3X_1 + 5X_2 + 11X_3 + X_4 + X_5 \quad (5)$$

The values of $F(X)$ at the critical true cells $\{ \overline{X_1} X_2 X_3 \overline{X_4} \overline{X_5}, X_1 \overline{X_2} X_3 \overline{X_4} X_5, X_1 \overline{X_2} X_3 X_4 \overline{X_5} \}$ are {16, 15, 15}, which indicates that the minimum value of $F(X)$ for a true vector is 15. The values of $F(X)$ at the critical false cells $\{ X_1 X_2 \overline{X_3} X_4 X_5, \overline{X_1} \overline{X_2} X_3 X_4 X_5, X_1 \overline{X_2} X_3 \overline{X_4} \overline{X_5} \}$ are {10, 13, 14}, which indicates that the maximum value of $F(\overline{X})$ for a false vector is 14 (strictly less than 15). This means that true vectors (cells) of the function are linearly-separable from false ones, and there is a gap or range [14, 15] in which a threshold T might be situated. We can take T=15 together with a set of weights {3, 5, 11, 1, 1}. Our calculations demonstrate the well-known fact that the weights and threshold of a threshold function are not necessarily unique [16].

c) Reliability Calculation

Consider the Coherent threshold system H (5 ; p ; 2, 3, 5, 1, 1 ; 8). The reliability of the system can be obtained by the recursive relation shown in

equation (6) subject to the boundary conditions in equation (7). The best policy to decompose the system is by arranging the weights in a descending order starting from the largest weight [17].

$$R(n ; \mathbf{p} ; \mathbf{W} ; T) = q_i R(n - 1 ; \mathbf{p}/p_i ; \mathbf{W}/W_i ; T) + p_i R(n - 1 ; \mathbf{p}/p_i ; \mathbf{W}/W_i ; T - W_i) \quad (6)$$

$$R(n ; \mathbf{p} ; \mathbf{W} ; T) = 1 \quad \text{if } 0 \geq T \quad (7a)$$

$$R(n ; \mathbf{p} ; \mathbf{W} ; T) = 0 \quad \text{if } \sum_{i=1}^n W_i < T \quad (7b)$$

The reliability for our running example with H (5 ; p ; 2, 3, 5, 1, 1 ; 8) (using our first set of weights and threshold) can be obtained by the recursive relation (6) together with the boundary conditions (7). We make decomposition first w.r.t. a component with the largest weight. Therefore, we make the decomposition w.r.t. the ordered elements 3, 2, 1, 4, and 5. The following computations mimic the growth and then shrinkage of a recursion stack for a computer implementation.

$$R(5 ; p_1, p_2, p_3, p_4, p_5 ; 2, 3, 5, 1, 1 ; 8) = q_3 R(4 ; p_1, p_2, p_4, p_5 ; 2, 3, 1, 1 ; 8) + p_3 R(4 ; p_1, p_2, p_4, p_5 ; 2, 3, 1, 1 ; 3),$$

$$R(4 ; p_1, p_2, p_4, p_5 ; 2, 3, 1, 1 ; 8) = 0,$$

$$R(4 ; p_1, p_2, p_4, p_5 ; 2, 3, 1, 1 ; 3) = q_2 R(3 ; p_1, p_4, p_5 ; 2, 1, 1 ; 3) + p_2 R(3 ; p_1, p_4, p_5 ; 2, 1, 1 ; 0),$$

$$R(3 ; p_1, p_4, p_5 ; 2, 1, 1 ; 3) = q_1 R(2 ; p_4, p_5 ; 1, 1 ; 3) + p_1 R(2 ; p_4, p_5 ; 1, 1 ; 1),$$

$$R(3 ; p_1, p_4, p_5 ; 2, 1, 1 ; 0) = 1,$$

$$R(2 ; p_4, p_5 ; 1, 1 ; 3) = 0,$$

$$\begin{aligned}
 R(2; p_4, p_5; \mathbf{1}, 1; 1) &= q_4 R(1; p_5; 1; 1) + p_4 R(1; p_5; 1; 0), \\
 R(1; p_5; 1; 0) &= 1, \\
 R(1; p_5; \mathbf{1}; 1) &= q_5 R(1; ; ; 1) + p_5 R(1; ; ; 0) = q_5 (0) + p_5 (1) = p_5, \\
 R(2; p_4, p_5; 1, 1; 1) &= q_4 p_5 + p_4, \\
 R(3; p_1, p_4, p_5; 2, 1, 1; 3) &= p_1(q_4 p_5 + p_4), \\
 R(4; p_1, p_2, p_4, p_5; 2, 3, 1, 1; 3) &= q_2 (p_1(q_4 p_5 + p_4)) + p_2, \\
 R(5; p_1, p_2, p_3, p_4, p_5; 2, 3, 5, 1, 1; 8) &= p_3 (q_2 (p_1(q_4 p_5 + p_4)) + p_2). \tag{8a}
 \end{aligned}$$

The reliability for our running example with $H(5; p; 3, 5, 11, 1, 1; 15)$ (using our second set of weights and threshold) can be obtained by the recursive relation (6) together with the boundary conditions (7). We again make the decomposition w.r.t. the ordered elements 3, 2, 1, 4, and 5.

$$\begin{aligned}
 R(5; p_1, p_2, p_3, p_4, p_5; 3, 5, \mathbf{11}, 1, 1; 15) &= q_3 R(4; p_1, p_2, p_4, p_5; 3, 5, 1, 1; 15) + \\
 & p_3 R(4; p_1, p_2, p_4, p_5; 3, 5, 1, 1; 4), \\
 R(4; p_1, p_2, p_4, p_5; 3, 5, 1, 1; 11) &= 0, \\
 R(4; p_1, p_2, p_4, p_5; 3, \mathbf{5}, 1, 1; 4) &= \\
 & q_2 R(3; p_1, p_4, p_5; 3, 1, 1; 4) + p_2 R(3; p_1, p_4, p_5; 3, 1, 1; -1), \\
 R(3; p_1, p_4, p_5; \mathbf{3}, 1, 1; 4) &= q_1 R(2; p_4, p_5; 1, 1; 4) + p_1 R(2; p_4, p_5; 1, 1; 1), \\
 R(3; p_1, p_4, p_5; 3, 1, 1; -1) &= 1, \\
 R(2; p_4, p_5; 1, 1; 4) &= 0, \\
 R(2; p_4, p_5; \mathbf{1}, 1; 1) &= q_4 R(1; p_5; 1; 1) + p_4 R(1; p_5; 1; 0), \\
 R(1; p_5; 1; 0) &= 1, \\
 R(1; p_5; \mathbf{1}; 1) &= q_5 R(1; ; ; 1) + p_5 R(1; ; ; 0) = q_5 (0) + p_5 (1) = p_5, \\
 R(2; p_4, p_5; 1, 1; 1) &= q_4 p_5 + p_4, \\
 R(3; p_1, p_4, p_5; 3, 1, 1; 4) &= p_1(q_4 p_5 + p_4), \\
 R(4; p_1, p_2, p_4, p_5; 3, 5, 1, 1; 4) &= q_2 (p_1(q_4 p_5 + p_4)) + p_2, \\
 R(5; p_1, p_2, p_3, p_4, p_5; 3, 5, 11, 1, 1; 15) &= p_3 (q_2 (p_1(q_4 p_5 + p_4)) + p_2). \tag{8b}
 \end{aligned}$$

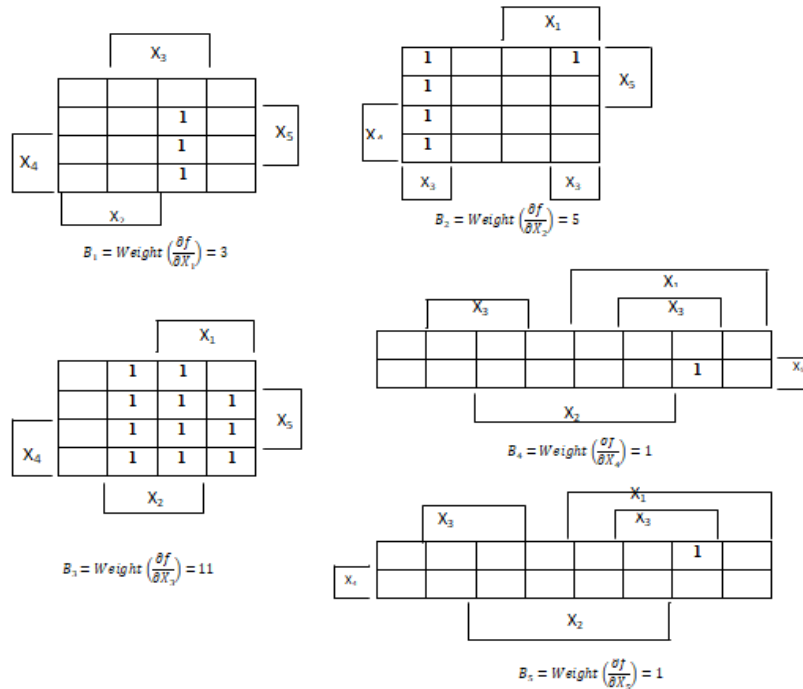


Fig. 4. Calculation of the Banzhaf indexes by using map folding to 'differentiate' the switching function of success and then calculating the weight of the obtained 'derivative'

We obtain the same expression of system reliability in (8a) and (8b), irrespective of the differences in the set of weights and threshold used. This expression consists of three terms, exactly the same number of terms in the Boolean domain in (4), a manifestation of the fact that a threshold function is shellable [17,19]. In fact, we could have applied the Reflection Law twice (or any more elaborate disjointing procedure [12]) to (4) to obtain the following probability-ready expression (PRE) [12].

$$f(X_1, X_2, X_3, X_4, X_5) = X_3 (X_2 \vee X_1 \overline{X_2} (\overline{X_4} X_5 \vee X_4)) \quad (4b)$$

The procedure for applying (6) and (7) to derive (8a) or (8b) could be pictorially visualized via a Mason signal flow graph that has the form of a reduced ordered binary decision diagram (ROBDD) [12,16-21]. Such a visualization is accomplished via a sequence of four figures (Fig. 5 to Fig. 8). The result in (8a), (8b), or (4a) could be visualized also on a Karnaugh map with disjoint loops (called a probability map, if the input switching variables are replaced by their expectations) as the one in Fig. 9 [36,37].

In passing, we note that any recursive function should not recur indefinitely (in an endless infinite loop) but must terminate in some non-recursive

cases. To the best of our knowledge, Rushdi [14] was the first to take this into consideration in the context of two-dimensional recursive formulation of reliability problems, through the use of what he termed ‘boundary conditions’ to mimic the somewhat similar situation in problems of electromagnetics. These boundary conditions did not only terminate recursion in a finite number of steps, but they also served as markers or borders for the region of validity of the recursive relations. Following the seminal work in [14], many authors followed suite to establish the concept of boundary conditions for many reliability systems [12,16-21,38-53]. Subsequently, this concept was extended even to higher dimensions [54,55].

The reliability algorithm used herein is demonstrated for a very small example of five components only. It can be readily used to handle a threshold system of any size. Its result is validated via the PRE in equation (4b), and also through each of the Karnaugh-map representation and the SFG visualization. This result can also be hand-checked via the fact that it is a multi-affine expression of component reliabilities that has a correct ‘truth table’ [56]. This correctness might be proved by showing that $R = 1$ for each of the three minimal paths in (4), and $R = 0$ for each of the minimal cutsets in (4a).

	\emptyset	{1}	{1,1}	{2,1,1}	{2,3,1,1}	{2,3,5,1,1}
$T = -3$	Green	Green	Green	Green	Green	Green
$T = -2$	Green	Green	Green	Green	Green	Green
$T = -1$	Green	Green	Green	Green	Green	Green
$T = 0$	Green	Green	Green	Green	Green	Green
$T = 1$	Pink	Yellow	Yellow	Yellow	Yellow	Yellow
$T = 2$	Pink	Pink	Yellow	Yellow	Yellow	Yellow
$T = 3$	Pink	Pink	Pink	Yellow	Yellow	Yellow
$T = 4$	Pink	Pink	Pink	Pink	Yellow	Yellow
$T = 5$	Pink	Pink	Pink	Pink	Pink	Yellow
$T = 6$	Pink	Pink	Pink	Pink	Pink	Pink
$T = 7$	Pink	Pink	Pink	Pink	Pink	Pink
$T = 8$	Pink	Pink	Pink	Pink	Pink	Pink

Fig. 5. Distribution of nodes in the two-dimensional plane of threshold versus weights for the first solution of the running example. A yellow cell should contain a non-source node expressed recursively via (6), and hence should have two arrows incident on it that emanate from nodes in the column to its left. Other cells represent source nodes. These are green cells containing nodes of unity values according to the condition $\{0 \geq T\}$ in (7a), and pink cells containing nodes of zero values according to the condition $\{\sum_{i=1}^n W_i < T\}$ in (7b)

	\emptyset	{1}	{1, 1}	{2, 1, 1}	{2, 3, 1, 1}	{2, 3, 5, 1, 1}
$T = -3$	Green	Green	Green	Green	Green	Green
$T = -2$	Green	Green	Green	Green	Green	Green
$T = -1$	Green	Green	Green	Green	Green	Green
$T = 0$	Green	Green	Green	Green	Green	Green
$T = 1$	Pink	Yellow	Yellow	Yellow	Yellow	Yellow
$T = 2$	Pink	Pink	Yellow	Yellow	Yellow	Yellow
$T = 3$	Pink	Pink	Pink	Yellow	Yellow	Yellow
$T = 4$	Pink	Pink	Pink	Pink	Yellow	Yellow
$T = 5$	Pink	Pink	Pink	Pink	Pink	Yellow
$T = 6$	Pink	Pink	Pink	Pink	Pink	Pink
$T = 7$	Pink	Pink	Pink	Pink	Pink	Pink
$T = 8$	Pink	Pink	Pink	Pink	Pink	Yellow

Fig. 6. Locations of all nodes in the two-dimensional plane of threshold versus weights, which are involved in the computations of the first solution for the running example. A yellow cell in a certain column is replaced by exactly two nodes in the column to its left, one at the same horizontal level, and another at a level higher by an amount equal to the weight of the component w.r.t. which expansion is performed. Processing terminates at a green cell of unity value or a pink cell of zero value. These locations guide the construction of a signal flow graph (SFG) in the forthcoming Fig. 7, and with appropriate differences, guide the construction of the SFG in Fig. 8.

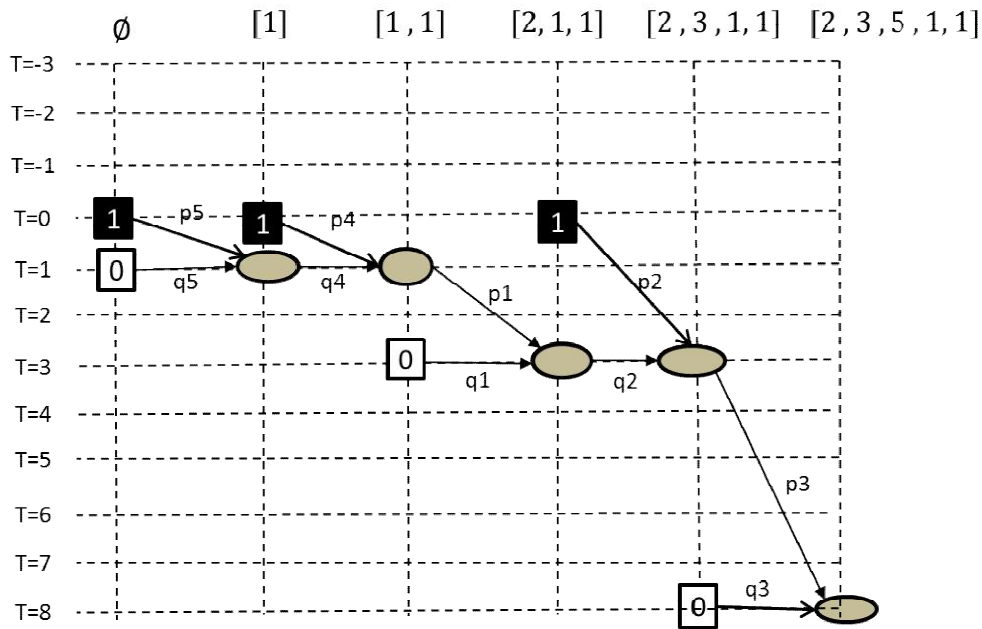


Fig. 7. A Mason signal flow graph (SFG) for computing the reliability for our running example with $H(5; p; 2, 3, 5, 1, 1; 8)$ (using our first set of weights and threshold) can be obtained by the recursive relation (6) together with the boundary conditions (7). The graph encompasses all equations leading to (8a) as node-defining equations. Simple application of Mason gain formula amounts to enumerating the three paths from the black source nodes to the single sink node, computing a non-factored version of (8a) by adding the gains of these paths.

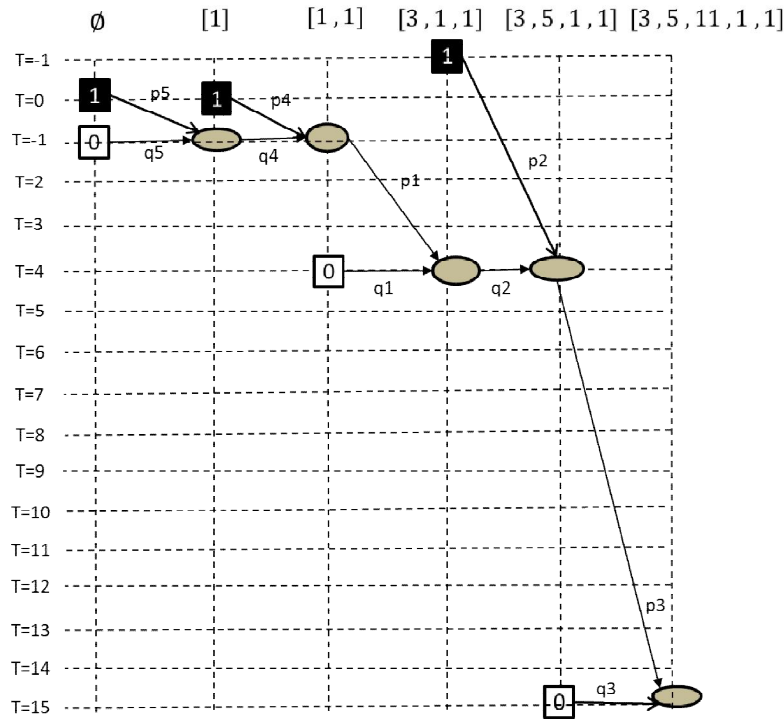


Fig. 8. A Mason signal flow graph (SFG) for computing the reliability for our running example with $H(5; p; 3, 5, 11, 1, 1; 15)$ (using our second set of weights and threshold) can be obtained by the recursive relation (6) together with the boundary conditions (7). The graph encompasses all equations leading to (8b) as node-defining equations. Simple application of Mason gain formula amounts to enumerating the three paths from the black source nodes to the single sink node, computing a non-factored version of (8b) by adding the gains of these paths. Despite the minor differences between the SFGs in Figs. 7 and 8, they yield exactly the same reliability expression.

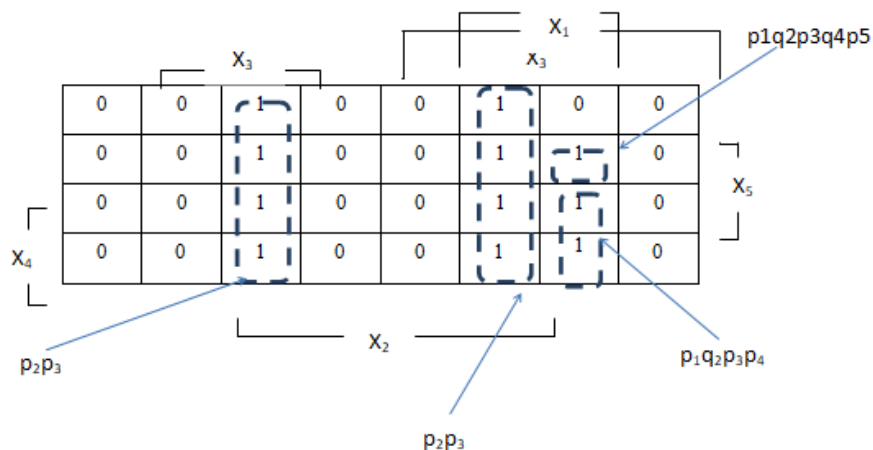


Fig. 9. System reliability obtained on a Karnaugh map treated as a probability map. The map loops are disjoint or non-overlapping. The loop p_2p_3 covers eight logically contiguous cells though it is split into two visually separated areas. The switching variables of the input domain are replaced by their expectations in the loop expressions.

3. CONCLUSIONS

The threshold system model (also called the weighted k-out-of-n:G system model) is used herein to analyze the reliability of a home-scale microgrid system. The system success is expressed as a threshold switching (Boolean) function, whose expectation (expected value) is the probability that the system works well, i.e., the system reliability. The present analysis aims to find the symbolic reliability and hence the relative importance of each component of the system.

COMPETING INTERESTS

The authors have declared that no competing interests exist.

REFERENCES

1. Peyghami S, Wang H, Davari P, Blaabjerg F. Mission-Profile-Based System-Level Reliability Analysis in DC Microgrids. *IEEE Trans. Ind. Appl.* 2019;55(5):5055–5067. DOI: 10.1109/TIA.2019.2920470
2. Bani-Ahmed A, Rashidi M, Nasiri A, Hosseini H. Reliability Analysis of a Decentralized Microgrid Control Architecture. *IEEE Trans. Smart Grid.* 2019;10(4):3910–3918. DOI: 10.1109/TSG.2018.2843527
3. Adefarati T, Bansal RC, Justo JJ. Reliability and economic evaluation of a microgrid power system. *Energy Procedia.* 2017;142:43–48. DOI: 10.1016/j.egypro.2017.12.008
4. Adefarati T, Bansal RC. Reliability and economic assessment of a microgrid power system with the integration of renewable energy resources. *Appl. Energy.* 2017;206:911–933. DOI: 10.1016/j.apenergy.2017.08.228
5. Fritz K, Kurz N, Peterson E. The Necessity to Perform a ‘Traditional’ Fault Tree Analysis Process when Conducting a Model-based Safety Assessment. *SAE Int. J. Aerosp.* 2012;5(1):214–223. DOI: 10.4271/2012-01-2130
6. Costa PM, Matos MA. Reliability of distribution networks with microgrids. *IEEE Russ. Power Tech, PowerTech.* 2005;1–7. DOI: 10.1109/PTC.2005.4524611
7. Kennedy S. Reliability evaluation of islanded microgrids with stochastic distributed generation. *IEEE Power Energy Soc. Gen. Meet. PES 09;* 2009. DOI: 10.1109/PES.2009.5275731
8. Luo Y, Wang L, Zhu G, Wang G. Network analysis and algorithm of microgrid reliability assessment. *Asia-Pacific Power Energy Eng. Conf. APPEEC;* 2010. DOI: 10.1109/APPEEC.2010.5448798
9. Shi X, Member S, Bazzi AM, Raditional IIIT, Ree FAT. Fault Tree Reliability Analysis of a Micro-grid Using Monte Carlo Simulations. in *IEEE Power and Energy Conference at Illinois (PECI).* 2015;3–7.
10. Deb S, Ghosh D, Mohanta DK. Reliability analysis of PV cell, wind turbine and diesel generator by using Bayesian network. in *International Conference on Electrical, Electronics, and Optimization Techniques, ICEEOT.* 2016;2714–2719. DOI: 10.1109/ICEEOT.2016.7755188
11. Bansal R. Handbook of distributed generation: Electric power technologies, economics and environmental impacts; 2017.
12. Rushdi AM, Rushdi MA. Switching-Algebraic Analysis of System Reliability in *Advances in reliability and system engineering,* Springer International Publishing AG. 2017;139–161.
13. Rackwitz R. Reliability analysis and prediction, a methodology oriented treatment. *Struct. Saf.* 1993;12(3):245–246. DOI: 10.1016/0167-4730(93)90007-n
14. Rushdi AM. Utilization of symmetric switching functions in the computation of k-out-of-n system reliability. *Microelectronics and Reliability.* 1986;26(5):973–987. DOI: 10.1016/0026-2714(86)90239-8
15. Lu Z, Liu W. Reliability evaluation of STATCOM based on the k-out-of-n: G model. *Int. Conf. Power Syst. Technol. POWERCON.* 2006;2006:1–6. DOI: 10.1109/ICPST.2006.321765
16. Rushdi AM. Threshold systems and their reliability. *Microelectronics and Reliability.* 1990;30(2):299-312.
17. Rushdi AM, Alturki AM. Reliability of coherent threshold system. *J. Appl. Sci.* 2015;15(3):431–443. DOI: 10.3923/jas.2015.431.443
18. Rushdi AM, Bjaili HA. An ROBDD algorithm for the reliability of double-threshold systems. *Journal of Advances in Mathematics and Computer Science.* 2016;7:1-7.
19. Rushdi AM, Alturki AM. Novel representations for a coherent threshold reliability system: a tale of eight signal ow

- graphs. Turkish Journal of Electrical Engineering & Computer Sciences. 2018;26(1):257-69.
20. Muktiadji RF, Rushdi AM. Reliability analysis of boost converters connected to a solar panel using a Markov approach. Journal of Energy Research and Reviews. 2021;7(1):29-42.
 21. Uswarman R, Rushdi AM. Reliability evaluation of rooftop solar photovoltaics using coherent threshold systems. Journal of Engineering Research and Reports. 2021;20(2):32-44.
 22. Serkan E, Yazgi Tutuncu G. Reliability evaluation of linear consecutive-weighted-k-out-of-n:F system. Asia-Pacific J. Oper. Res. 2009;26(6):805–816. DOI: 10.1142/S0217595909002481
 23. Zhuang X, Yu T, Sun Z, Song K. Reliability and capacity evaluation of multi-performance multi-state weighted K --out-of-n systems. Commun. Stat. Simul. Comput. 2020;1–17. DOI: 10.1080/03610918.2020.1788590
 24. Song X, Zhai Z, Guo Y, Zhu P, Han J. Approximate analysis of multi-state weighted k-out-of-n systems applied to transmission lines. Energies. 2017;10(11):1–16. DOI: 10.3390/en10111740
 25. Rushdi MA, Rushdi AA, Dief TN, Halawa AM, Yoshida S, Schmehl R. Power prediction of airborne wind energy systems using multivariate machine learning. Energies. 2020;13(2367):1-23.
 26. Rushdi MA, Dief TN, Halawa AM, Yoshida S. System identification of a 6 m2 kite power system in fixed-tether length operation. International Review of Aerospace Engineering. 2020;13(4):150-8.
 27. Salma V, Friedl F, Schmehl R. Improving reliability and safety of airborne wind energy systems. Wind Energy. 2020;23(2):340-356.
 28. Rushdi MA, Dief TN, Yoshida S, Schmehl R. Towing test data set of the Kyushu University kite system. Data. 2020;5(69):1-18.
 29. Rushdi AM. Map derivation of the minimal sum of a switching function from that of its complement. Microelectronics and Reliability. 1985;25(6):1055-1065.
 30. Rushdi AM. Map differentiation of switching functions. Microelectronics and Reliability. 1986;26(5):891-907.
 31. Rushdi AM. On computing the syndrome of a switching function. Microelectronics and Reliability. 1987;27(4):703-716.
 32. Rushdi MA, Rushdi AM, Zarouan M, Ahmad W. Satisfiability in intuitionistic fuzzy logic with realistic tautology. Kuwait Journal of Science. 2018;45(2):15-21.
 33. Alturki AM, Rushdi AM. Weighted voting systems: A threshold-Boolean perspective. Journal of Engineering Research. 2016;1(4):1-19.
 34. Rushdi AM, Ba-Rukab OM. Calculation of Banzhaf voting indices utilizing variable-entered Karnaugh maps. Journal of Advances in Mathematics and Computer Science. 2017;20(4):1-17.
 35. Rushdi AM, Ba-Rukab OM. Translation of Weighted Voting Concepts to the Boolean Domain: The Case of the Banzhaf Index. Chapter 10 in Advances in Mathematics and Computer Science Vol. 2. Book Publisher International, Hooghly, West Bengal, India. 2019:122-140.
 36. Hurley RB. Probability maps. IEEE Transactions on Reliability. 1963;12(3):39-44.
 37. Rushdi AM. Symbolic reliability analysis with the aid of variable-entered Karnaugh maps. IEEE Transactions on Reliability. 1983;32(2):134-139.
 38. Rushdi AM, Dehlawi FM. Optimal computation of k-to-l-out-of-n system reliability. Microelectronics and Reliability. 1987;27(5):875-896, Erratum: ibid. 1988;28(4):671.5):875-896.
 39. Rushdi AM. Reliability of k-out-of-n Systems. Chapter 6 in K. B. Misra, New Trends in System Reliability Evaluation, Fundamental Studies in Engineering, Elsevier Science Publishers, Amsterdam, The Netherlands. 1993;16:185-227.
 40. Zuo M, Chiovelli S, Huang J. Reliability evaluation of furnace systems. Reliability Engineering & System Safety. 1999;65(3):283-287.
 41. Huang J, Zuo MJ, Wu Y. Generalized multi-state k-out-of-n: G systems. IEEE Transactions on reliability. 2000;49(1):105-111.
 42. Lin D, Zuo MJ. Reliability evaluation of a linear k-within-(r, s)-out-of-(m, n): F lattice system. Probability in the Engineering and Informational Sciences. 2000;14(4):435-443.
 43. Yamamoto H, Akiba T. A recursive algorithm for the reliability of a circular connected-(r, s)-out-of-(m, n): F lattice system. Computers & Industrial Engineering. 2005;49(1):21-34.

44. Yamamoto H, Zuo MJ, Akiba T, Tian Z. Recursive formulas for the reliability of multi-state consecutive-k-out-of-n: G systems. *IEEE Transactions on Reliability*. 2006;55(1):98-104.
45. Zuo MJ, Tian Z, Huang HZ. An efficient method for reliability evaluation of multistate networks given all minimal path vectors. *IIE Transactions*. 2007;39(8):811-817.
46. Tian Z, Li W, Zuo MJ. Modeling and reliability evaluation of multi-state k-out-of-n systems. In *Recent Advances in Reliability and Quality in Design*, Springer, London.2008;31-56.
47. Tian Z, Zuo MJ, Yam RC. Multi-state k-out-of-n systems and their performance evaluation. *IIE Transactions*. 2008;41(1):32-44.
48. Rushdi AM. Partially-redundant systems: Examples, reliability, and life expectancy, *International Magazine of Advanced Computer Science and Telecommunications*. 2010;1(1):1–13
49. Rushdi AM, Ghaleb FA. A tutorial exposition of semi-tensor products of matrices with a stress on their representation of Boolean functions. *Journal of King Abdulaziz University: Computing and Information Technology Sciences*. 2016;5(1):3-30.
50. Nakamura T, Yamamoto H, Shinzato T, Xiao X, Akiba T. Reliability of a circular connected-(1, 2)-or-(2, 1)-out-of-(m, n): F lattice system with identical components. *IEICE Transactions on Fundamentals of Electronics, Communications and Computer Sciences*. 2017;100(4):1029-1036.
51. Rushdi AM. Utilization of symmetric switching functions in the symbolic reliability analysis of multi-state k-out-of-n systems. *International Journal of Mathematical, Engineering and Management Sciences (IJMEMS)*. 2019;4(2):306-326.
52. Rushdi AM, Alturki AM. Representations of a coherent reliability system via signal flow graphs, *Journal of King Abdulaziz University: Engineering Sciences*. 2020;31(1):3–18.
53. Rushdi AM, AlHuthali SA, AlZahrani NA, Alsayegh AB. Reliability analysis of binary-imaged generalized multi-State k-out-of-n systems. *International Journal of Computer Science and Network Security (IJCSNS)*. 2020;20(9):251-264.
54. Amari SV, Zuo MJ, Dill GO. (kn) algorithms for analyzing repairable and non-repairable k-out-of-n: G systems. In *Misra KB (Editor), Handbook of Performability Engineering*, Springer, London. 2008;309-320.
55. Rushdi MAM, Ba-Rukab OM, Rushdi AM. Multi-dimensional recursion relations and mathematical induction techniques: The case of failure frequency of k-out-of-n systems *Journal of King Abdulaziz University: Engineering Sciences*. 2016;27(2):15–31.
56. Rushdi AM. How to hand-check a symbolic reliability expression. *IEEE Transactions on Reliability*. 1983;5:402-408.

© 2021 Hidayat and Rushdi; This is an Open Access article distributed under the terms of the Creative Commons Attribution License (<http://creativecommons.org/licenses/by/4.0>), which permits unrestricted use, distribution, and reproduction in any medium, provided the original work is properly cited.

Peer-review history:

*The peer review history for this paper can be accessed here:
<http://www.sdiarticle4.com/review-history/67300>*